

# Electron-induced delayed desorption of solid argon doped with methane

I.V. Khyzhniy<sup>1</sup>, S.A. Uytunov<sup>1</sup>, M.A. Bludov<sup>1</sup>, E.V. Savchenko<sup>1</sup>, and V.E. Bondybey<sup>2</sup>

<sup>1</sup>*B. Verkin Institute for Low Temperature Physics and Engineering of the National Academy of Sciences of Ukraine  
47 Nauky Ave., Kharkiv 61103, Ukraine  
E-mail: savchenko@ilt.kharkov.ua*

<sup>2</sup>*Lehrstuhl für Physikalische Chemie II TUM, Garching b. Munich 85747, Germany*

Received March 12, 2019, published online May 28, 2019

The total yield of particles desorption from solid Ar doped with CH<sub>4</sub> under irradiation with an electron beam was studied at 5 K. The measurements were carried out at a CH<sub>4</sub> concentration of 1 and 5%. The effect of explosive delayed desorption from the surface of argon matrix was discovered in both mixtures. With a higher concentration of CH<sub>4</sub>, it appeared at lower doses and was more pronounced. Two types of self-oscillations were observed: long-period bursts (on a time scale of about 25 min) and short-period oscillations (of about 10 s). In pure solid Ar delayed desorption was not observed despite the accumulation of a significant number of excess electrons, exceeding their number in mixtures of Ar and CH<sub>4</sub> as it was found by measurements of thermally stimulated exoelectron emission. This finding discards the model of Coulomb explosion for the phenomenon detected. In this paper we focused on the role of hydrogen (one of the radiolysis products) in delayed desorption. The formation of atomic hydrogen in the matrix was traced via cathodoluminescence by the emission band of the excimer Ar<sub>2</sub>H\* at 166 nm. Desorption of excited hydrogen atoms in the excited state was detected by the Ly- $\alpha$  emission line. A decrease of the Ar<sub>2</sub>H\* band intensity at higher concentration of CH<sub>4</sub> was found evidencing bleaching these centers likely due to recombination of H atoms with energy release and formation of molecular hydrogen. The data obtained give additional evidence in favor of the hypothesis that the exothermic reactions of radiolysis products serve as a stimulating factor for delayed desorption.

Keywords: CH<sub>4</sub> in Ar matrix, electron irradiation, explosive delayed desorption, cathodoluminescence, self-oscillations.

## Introduction

Solid methane being an important constituent of Interstellar Medium and Solar System has attracted considerable interest in astrophysics community [1–5]. Properties of methane, their transformation caused by the continuous radiation of outer space, and physicochemical processes became the topic of a large body of research. Numerous techniques have been introduced to simulate radiation-induced processes in the laboratory [6]. Various types of ionizing radiation were used to study radiation behavior of methane and methane-rich ices, e.g., ions [7–14], electrons [15–21] and photons [19,22–24]. Essential radiation-induced modification of solid methane was detected with appearance of a number of products (H, H<sub>2</sub>, CH<sub>3</sub>, CH<sub>2</sub>, CH, C<sub>2</sub>H<sub>6</sub>, etc.). It was shown that the initial step of the chemical transformation appears to be generation of the methyl radical CH<sub>3</sub> and atomic hydrogen (CH<sub>4</sub> → CH<sub>3</sub> + H). As shown in [19], a wealth of highly unsaturated species are

formed via the successive loss of hydrogen atoms. The detection of the radiolysis products by FTIR spectroscopy allowed the authors to construct a model of chemical reactions describing radiation-induced modification of methane. The most abundant product at the end of electron beam irradiation was ethane C<sub>2</sub>H<sub>6</sub> (59% of the total carbon consumed from methane in the experiments [19]). Note that generation of charged species and their neutralization were not considered in [19].

Special point of interest to radiation effects in solid methane is its interaction with neutrons. In view of high efficiency of the conversion of short wavelength neutrons to long wavelength ones, which is ~ 3.5 times higher than that achieved in liquid hydrogen based moderators, solid methane is proven to be the most promising material for cold moderators [25]. However its use in cryogenic moderators encounters difficulties when dealing with intense neutron flux. It appeared that a neutron flux irradiating a methane moderator, can cause spontaneous release of ac-

cumulated energy, rapid heating followed by hydrogen expansion and moderator destruction [25,26]. This, so-called “burp” effect — self-accelerated heating process, detected by J. Carpenter, attracted much attention in the neutron community and a number of thorough studies were performed, e.g., [26–28]. The results of this research provided support of Carpenter’s model according to which energy accumulated and stored in the form of reactive species (H, CH<sub>3</sub>...) upon low-temperature irradiation is then released by thermally activated diffusion and subsequent reactions [25]. Gas chromatography analysis performed in [25] after one week’s irradiation and vaporization of the moderator container content indicated about 5.4 mol % H<sub>2</sub>, 2.3 mol % C<sub>2</sub>H<sub>6</sub>, with smaller concentrations of other hydrocarbons. This finding supports the suggestion that the exothermic reactions of radical recombination: H + H → H<sub>2</sub> and CH<sub>3</sub> + CH<sub>3</sub> → C<sub>2</sub>H<sub>6</sub> serve as an energy source in the process under discussion. Carpenter’s model described the phenomenon using one activation energy  $E_{\text{act}} = 155$  K. Further experiments [28,29] pointed to more complex scenario. It was suggested [28] that more than one process underlies the observed phenomenon. This suggestion was supported by the experiments performed with electron beam applying current activation spectroscopy technique [20,29,30]. It was found that there are two channels of relaxation — low-temperature one operating in the temperature range 10–20 K and “high”-temperature relaxation channel which comes into play upon reaching 40 K. Maxima of thermally stimulated exoelectron emission (TSEE) were detected in those ranges as well as yields of thermally stimulated post-desorption (TSpD). Moreover explosive particle desorption and flash of photons were detected upon irradiation of methane at 5 K with the delay of an hour with respect to the start of irradiation by 1 keV electron beam of 3 mA/cm<sup>2</sup> current density [31,32]. The outburst of particles was preceded by oscillations of particles desorption of increasing amplitude. Note that delayed desorption of

similar kind was observed under exposure of methane film to 9.0 MeV  $\alpha$ -particles and 7.3 MeV protons [8]. However in that study authors did not detect regular oscillations.

Here we present our further research on this effect. To get more insight into the phenomenon we investigated radiation effects induced by an electron beam in solid Ar doped with CH<sub>4</sub>. Energy transfer to dopant in Ar matrix is quite efficient because Ar free excitons (12.1 eV [33]) fall into the absorption band of CH<sub>4</sub> molecule [34]. Taking into account that in a presence of energetic electrons ionization process would be of importance we chose solid argon as the matrix in view of high ionization potential  $I$  of Ar ( $I = 15.7$  eV) exceeding the ionization potential of methane of CH<sub>4</sub> ( $I = 12.6$  eV). This ratio of ionization potentials facilitates the formation of CH<sub>4</sub><sup>+</sup> and other ionic species, e.g., H<sup>+</sup>, CH<sub>3</sub><sup>+</sup>, C<sub>2</sub>H<sub>6</sub><sup>+</sup>, in Ar matrix. Neutralization of CH<sub>4</sub><sup>+</sup> proceeds via dissociative recombination resulting in the appearance of radiolysis products. Substitutional site in Ar lattice is about 0.376 nm [35] that is close to the kinetic diameter of CH<sub>4</sub> (0.380 nm) and the methane molecules can occupy substitutional site at low concentrations of dopant. But starting with a methane concentration of 3%, the argon lattice in the vicinity of the impurity is modified and at higher concentration about 20% a two-phase system is obtained [36]. Taking this into account, the concentration of CH<sub>4</sub> should not be too high. On the other hand, it should not fall into the two-phase region. So, we have chosen concentrations of 1 and 5% CH<sub>4</sub>. For these systems delayed explosive-like particle desorption was also detected followed by oscillations of particles emission.

## Experimental

The experimental procedures have been described in detail in Sec. 7 of Ref. 6. In the following, we give a brief account of the procedures. Figure 1 represents a schematic sketch of the experimental set-up.

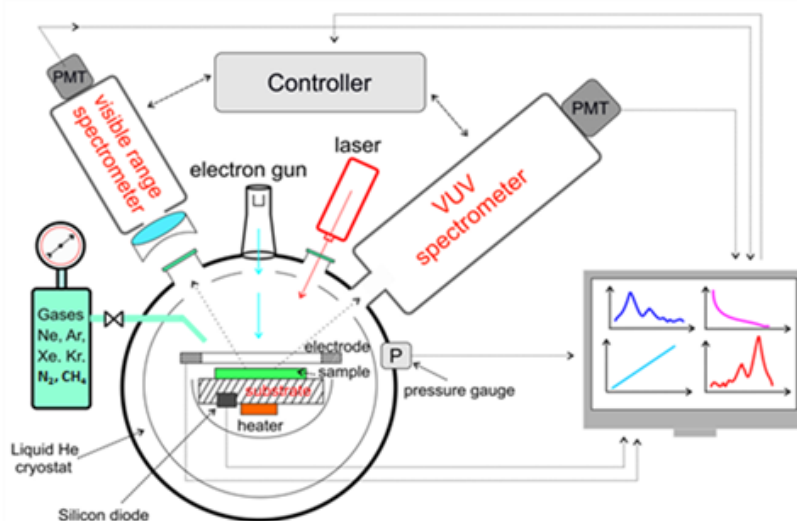


Fig. 1. Scheme of the experimental set-up for emission spectroscopy of solidified gases.

Mixture of Ar and CH<sub>4</sub> of defined concentration was performed in the gas-handling system which was heated and degassed before each experiment. We used Ar gas (99.998%) and CH<sub>4</sub> gas (99.97%) without further purification. Films of solid Ar doped with methane were grown by deposition of a certain amount of gas onto a cooled to LHe temperature Cu substrate mounted in a high-vacuum chamber with a base pressure of  $< 10^{-7}$  Torr. A LHe cryostat was used to ensure a stable temperature. 25  $\mu\text{m}$  thick unannealed films were used in these experiments. The sample temperature was controlled during the entire experiment with a Si sensor.

The irradiation was performed in dc regime with subthreshold energy electrons ( $E_e < 1.7$  keV) to avoid the knock-on sputtering. In most of the experiments, the electron beam energy  $E_e$  was set to 1.5 keV with the current density of  $2.5 \text{ mA/cm}^2$ . The beam covered the icy film with an area of  $1 \text{ cm}^2$ . The sample heating under electron beam did not exceed 0.4 K.

Cathodoluminescence (CL) spectra were registered simultaneously in the VUV range and in the visible one. The dose deposited by irradiation was determined from the exposure time for a constant beam intensity. Particle desorption under beam was monitored with an ionization detector (a Bayard-Alpert gauge) throughout the entire experiment.

On completing irradiation we detected an “afteremission” current. Measurements of thermally stimulated relaxation emissions from solid Ar doped with CH<sub>4</sub> were started when the “afteremission” current had decayed to essentially zero. In these experiments we used heating with a constant rate of 5 K/min. Released from shallow traps electrons being promoted to the conduction band either neutralize positively charged centers or escape from the film yielding TSEE current. Stimulated currents were detected with an electrode kept at a small positive potential  $V_F = +9$  V and connected to the current amplifier. TSEE curves reflect the distribution of electron traps (defects) in the sample and provide an information on the trap levels in grown and irradiated samples as well as charge accumulation. Figure 2 illustrates TSEE yields from pure and doped Ar matrix. The low-temperature peak at 8 K in doped samples corresponds to the most shallow traps induced by dopants. The next wide peak at about 16 K represents a multipeak curve with unresolved structure incorporating components related to different defects of structure. In pure methane, the second peak has been observed at 18 K [30].

It can be seen that the number of defects in the temperature range of 15–35 K in Ar doped with 1% of CH<sub>4</sub> is almost the same as their content in the pure matrix. In the temperature range below 15 K, the number of defects in doped Ar is significantly reduced and their distribution differs from that in the pure matrix. An important point is that the number of excess electrons accumulated in pure solid Ar exceeds their number in mixtures of Ar with CH<sub>4</sub> as seen from Fig. 2.

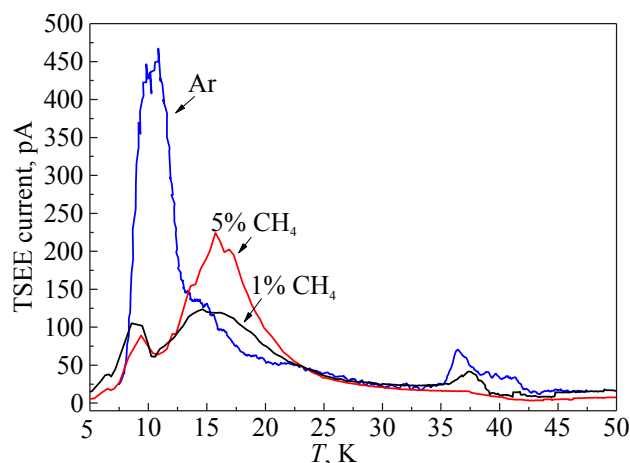
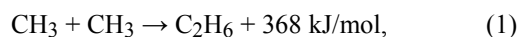


Fig. 2. TSEE from pure Ar and Ar doped with CH<sub>4</sub> of different concentrations.

Note that all measurements, both while the beam is on, and after its shutdown and subsequent heating, were performed in the dynamic pumping mode. Pumping out was carried out by LHe cryogenic pump and magnetic discharge pump. All parameters during the entire experiment were controlled by a special program developed for current experiments.

## Results and discussion

The most likely sources of energy for explosive desorption at low temperatures are the exothermic recombination reactions of CH<sub>3</sub> radicals and hydrogen atoms [25]:



In this paper we focused on the role of hydrogen in the phenomenon of delayed desorption. The formation of atomic hydrogen in the matrix can be traced by the known emission band of the excimer Ar<sub>2</sub>H\*, which falls in the VUV range. The lowest resonant transition of a hydrogen atom in a gas is also in the VUV range — Lyman- $\alpha$  line at 121.6 nm. Therefore, we will present the VUV spectra of CL of solid Ar doped with CH<sub>4</sub> and try to trace their connection to the delayed desorption. Typical CL spectrum of Ar matrix doped with 5% CH<sub>4</sub> is shown in Fig. 3.

The most intense feature of this spectrum at 127 nm is the well-known emission of molecular-type self-trapped excitons Ar<sub>2</sub>\*, corresponding to the transitions from  $1,3\Sigma$  states to a repulsive part of the ground state  $1\Sigma_g$  [33]. This band is also seen in the second order. The radiative states can be populated via both the processes of exciton self-trapping and the recombination of the self-trapped holes (Ar<sup>2+</sup>) with an electron. The efficiency of the recombination channel of luminescence was demonstrated in [37]. The weak feature near 109 nm stems from atoms and unrelaxed argon molecules desorbing in excited states.

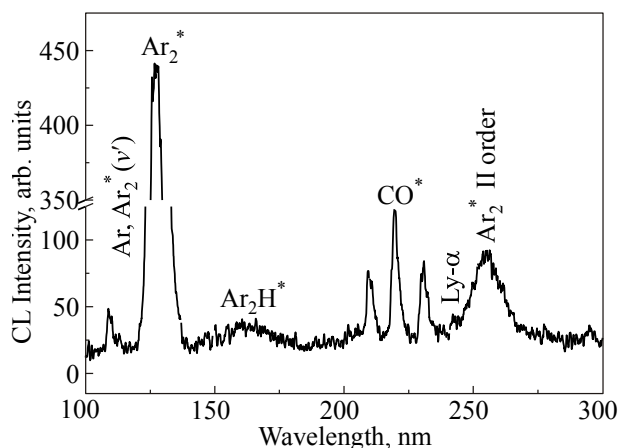


Fig. 3. VUV CL spectrum of solid Ar doped with 5% CH<sub>4</sub>.

These features are not resolved in the spectrum shown because the recording was made with a wide spectral slit to enable the detection of weak emissions. It should be noted that the addition of methane strongly quenches the matrix luminescence. The spectrum also contains impurity bands of CO (the Cameron system). The most interesting feature related to the present study is the excimer emission band near 166 nm, which corresponds to the emission of the Ar<sub>2</sub>H\* center at the transition to the repulsive part of the ground-state potential curve [38]. Most likely, the formation of this center occurs via neutralization of ionic hydride Ar<sub>2</sub>H<sup>+</sup>, similar to the process considered in [39] for the formation of Xe<sub>2</sub>H\* upon electron bombardment of the Xe–H<sub>2</sub> mixture. The observation of the Ar<sub>2</sub>H\* emission band in our experiment clearly indicates a rather efficient dissociation of CH<sub>4</sub> in the Ar matrix despite the “cage effect” and accumulation of atomic hydrogen. This effect can be expected because not only the decomposition of CH<sub>4</sub>, but also most chemical reactions of methane radiolysis products occur with the formation of hydrogen atoms. Intensity distribution in the spectrum varies with the CH<sub>4</sub> concentration. Figure 4 shows the VUV CL spectrum taken at the CH<sub>4</sub> concentration of 1%.

In addition to the features observed at 5% methane in Ar, a broad band appears at 184 nm. Its identification is not entirely clear at present. In solid Ar, even in earlier studies, e.g., [40,41], a wide emission band was recorded at 200 nm, the so-called third continuum. Analogs of this continuum were recorded in the gas [42–45] and liquid phase of argon [46]. In most of the studies, its origin was associated with transitions in ionic centers Ar<sub>2</sub><sup>+</sup> or the decay of Ar<sub>2</sub><sup>2+</sup>. It was underlined that several components of different origin contribute to the third continuum of Ar. One might assume that under the conditions of our experiment one of the components appears in the spectrum. Taking into account the uncertainty of the continuum at 184 nm identification and its low intensity in relation to the matrix’s own emission band (Ar<sub>2</sub>\*), we compared the ratio of the Ar<sub>2</sub>H\*

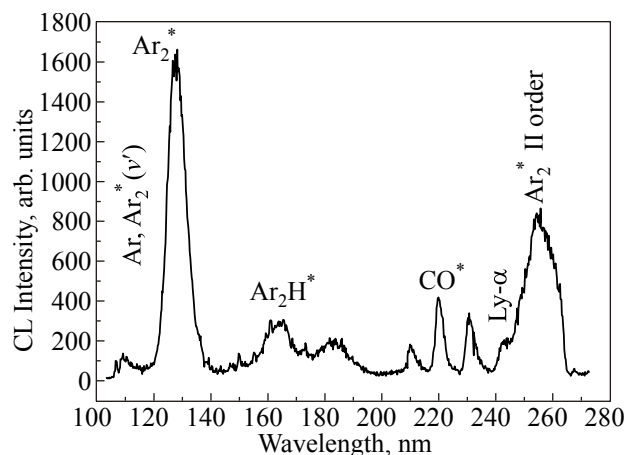


Fig. 4. VUV CL spectrum of solid Ar doped with 1% CH<sub>4</sub>.

band and Ar<sub>2</sub>\* band intensities in samples with a different CH<sub>4</sub> content. The ratio  $I(\text{Ar}_2\text{H}^*)/I(\text{Ar}_2^*)$  increased 5 times with decreasing methane concentration from 5 to 1%. This implies a more rapid depletion of atomic hydrogen at higher concentrations due to its diffusion followed by nonradiative recombination of the H radicals with the release of energy and the formation of molecular hydrogen.

In rare gas matrices the hydrogen atom occupies two types of sites — interstitial site and substitutional one [47]. The atoms occupying the interstitial sites are released at moderate heating, while the atoms trapped in the substitutional sites remain trapped at low temperatures [48]. It should be underlined that atoms produced by dissociation have an excess of kinetic energy facilitating local diffusion, while atoms which are in thermal equilibrium with the lattice appeared to be stable. So H··H spin pair diradicals with a distribution of internuclear distances > 0.7 nm were detected by ESR spectroscopy at LHe temperature [49].

First of all we checked if there is a burst of desorption upon irradiation with electron beam of pure Ar matrix. Irradiation performed with the same parameters of the beam during twice more time did not show any strong

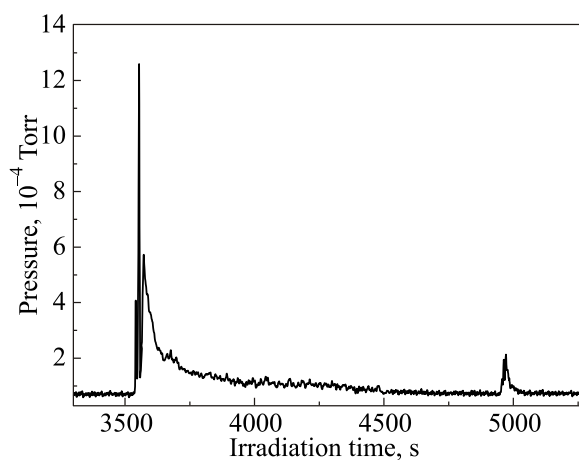


Fig. 5. Delayed explosive desorption of solid Ar doped with 1% CH<sub>4</sub>.

bursts. Monitoring of the electron-induced desorption from solid Ar doped with 1% of CH<sub>4</sub> already revealed the delayed desorption as shown in Fig. 5.

The first burst of desorption was observed about an hour after the start of irradiation. It resulted in the chamber pressure increasing by an order of magnitude. The process reoccurred after about 25 min but the second burst was much weaker and was accompanied by a slight drop in the chamber pressure. The structure of these bursts (the irradiation time dependence) is shown in Figs. 6(a) and (b).

The first burst of particles desorption is composed of three huge amplitude peaks spaced apart by more than 10 s each. The increase in the delayed desorption yield occurs much faster than its decay. The peaks of the second burst are of smaller amplitude. They are rising with a period of about 7 s and then fade out.

With a rise of CH<sub>4</sub> concentration to 5% the phenomenon of delayed desorption has become more pronounced as shown in Fig. 7.

When the electron beam is turned on desorption of particles begins at a low rate resulting in a moderate rise of pressure accompanying electronically stimulated desorption of Ar matrix. Signatures of desorbing excited Ar\* atoms and unrelaxed Ar<sub>2</sub><sup>\*</sup>(ν) molecules are seen in Figs. 3

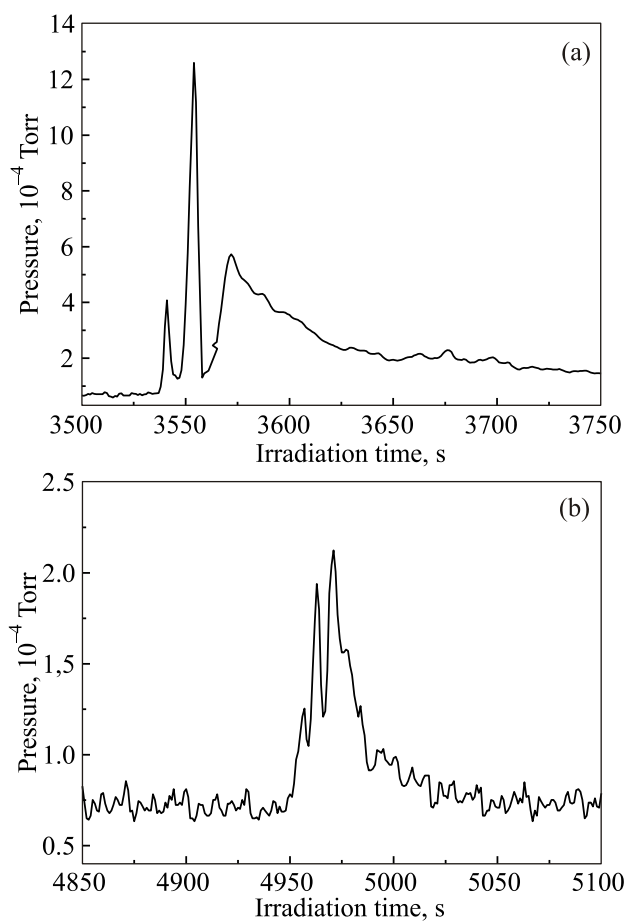


Fig. 6. Structure of the first (a) and second (b) bursts of particles from solid Ar doped with 1% CH<sub>4</sub>.

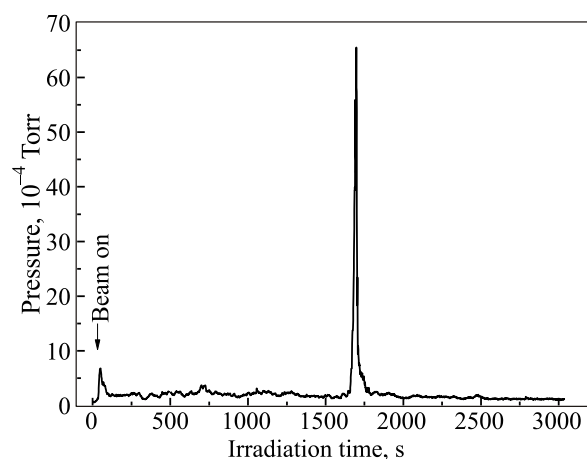


Fig. 7. Delayed explosive desorption from solid Ar doped with 5% CH<sub>4</sub>. Small peak at the beginning appeared when the beam current was brought to a stationary mode.

and 4 near 109 nm. Interestingly, in these spectra recorded before the burst of desorption, the Lyman- $\alpha$  line belonging to the hydrogen atoms desorbing in the excited state was recorded. It is visible in the second order of the spectra at 243 nm. After irradiation during half an hour, the desorption yield rises rapidly in explosive-like way by two orders of magnitude as can be seen in Fig. 7. The burst lasts for about 100 s and then desorption decreases to a steady state value. A most remarkable feature of this delayed desorption is that oscillations are appearing just before the burst and increasing in amplitude. They are seen also after the burst gradually decaying. The behavior of the total desorption yield in the burst range is shown in Fig. 8.

Appearing of such a pronounced burst with oscillations correlates with a decrease of the intensity of Ar<sub>2</sub>H\* band evidencing bleaching these centers likely due to recombination of H atoms with energy release and formation of molecular hydrogen.

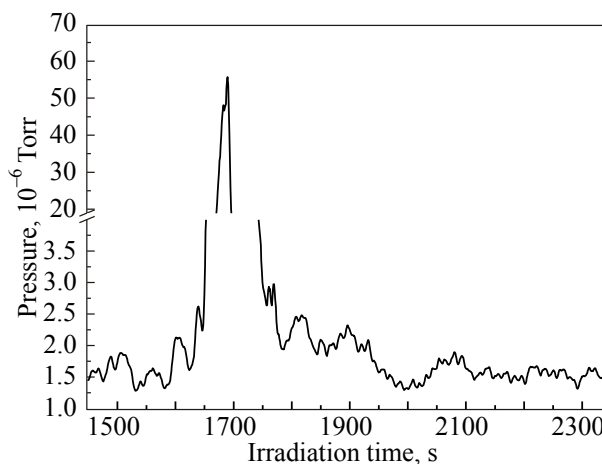


Fig. 8. Enlarged view of the burst area taken from solid Ar doped with 5% CH<sub>4</sub>.

Note that in pure solid methane a pressure increase by three orders of magnitude during the delayed burst and distinct long lasting oscillations with a period of 10 s were observed upon exposure to an electron beam [31,32]. The existence of two types of periodic processes: short-period oscillations of small amplitude and long-period strong bursts, implies the two systems are involved in the delayed desorption observed. The detected phenomenon is an example of radiation-induced self-oscillations similar to those considered in [50]. The data obtained discard the model of Coulomb explosion and provide additional proof in favor of the hypothesis that the exothermic reactions of radiolysis products serve as a stimulating factor for the delayed desorption upon electron irradiation. More systematic studies are required to understand in more detail the underlying processes.

### Acknowledgments

The authors cordially thank colleagues Giovanni Strazzulla, Oleg Kirichek, Vladimir Sugakov, Hermann Rothard, Peter Feulner and Jürgen Hauer for stimulating discussions.

1. R.N. Clark, R. Carlson, W. Grundy, and K. Noll, *Observed Ices in the Solar System*, in: *The Science of Solar System Ices; Astrophysics and Space Science Library*, M.S. Gudipati and J. Castillo-Rogez (eds.), Springer, New York (2012), Vol. 356, p. 3
2. K.I. Öberg, *Chem. Rev.* **116**, 9631 (2016).
3. Ch.K. Materese, D.P. Cruikshank, S.A. Sandford, H. Imanaka, and M. Nuevo, *Astrophys. J.* **812**, 150 (2015).
4. M.E. Brown, C.A. Trujillo, and D.L. Rabinowitz, *Astrophys. J.* **635**, L97 (2005).
5. D.P. Cruikshank, T.L. Roush, T.C. Owen, T.R. Geballe, C. de Bergh, B. Schmitt, R.H. Brown, and M.J. Bartholomew, *Scienc* **261**, 742 (1993).
6. M.A. Allodi, R.A. Baragiola, G.A. Baratta, M.A. Barucci, G.A. Blake, J.R. Brucato, C. Contreras, S.H. Cuyille, Ph. Boduch, D. Fulvio, M.S. Gudipati, S. Ioppolo, Z. Kaňuchová, A. Lignell, H. Linnartz, M.E. Palumbo, U. Raut, H. Rothard, F. Salama, E.V. Savchenko, E. Sciamma-O'Brien, G. Strazzulla, and G. Strazzulla, *Space Sci. Rev.* **180**, 101 (2013).
7. G. Foti, L. Calcagno, K. Sheng, and G. Strazzulla, *Nature* **310**, 126 (1984).
8. R.I. Kaiser, G. Eich, A. Gabrysch, and K. Roessler, *The Astrophys. J.* **484**, 487 (1997).
9. R.I. Kaiser and K. Roessler, *Astrophys. J.* **503**, 959 (1998).
10. C.F. Mejía, A.L.F. de Barros, V. Bordalo, E.F. da Silveira, P. Boduch, A. Domaracka, and H. Rothard, *Monthly Notices of the Royal Astronomical Society* **433**, 2368 (2013).
11. M.E. Palumbo, G.A. Baratta, D. Fulvio, M. Garozzo, O. Gomis, G. Leto, F. Spinella, and G. Strazzulla, *J. Phys.: Conf. Ser.* **101**, 012002 (2008).
12. R. Brunetto, M.A. Barucci, E. Dotto, and G. Strazzulla, *Astrophys. J.* **644**, 646 (2006).
13. F.A. Vasconcelos, S. Pilling, W.R.M. Rocha, H. Rothard, P. Boduch, and J.J. Ding, *Phys. Chem. Chem. Phys.* **19**, 12845 (2017).
14. A.L.F. de Barros, V. Bordalo, E. Seperuelo Duarte, E.F. da Silveira, A. Domaracka, H. Rothard, and P. Boduch, *Astronomy & Astrophysics A* **531**, 160 (2011).
15. T. Huang and W.H. Hamill, *J. Phys. Chem.* **78**, 2077 (1974).
16. C.J. Bennett, C.S. Jamieson, Y. Osamura, and R.I. Kaiser, *Astrophys. J.* **653**, 792 (2006).
17. M. Barberio, R. Vasta, P. Barone, G. Manicò, and F. Xu, *World J. Condens. Matter Phys.* **3**, 14 (2013).
18. B.M. Jones and R.I. Kaiser, *J. Phys. Chem. Lett.* **4**, 1965 (2013).
19. M.J. Abplanalp, B.M. Jones, and R.I. Kaiser, *Phys. Chem. Chem. Phys.* **20**, 543 (2018).
20. E. Savchenko, I. Khyzhniy, S. Uyutnov, M. Bludov, A. Barabashov, G. Gumenchuk, and V. Bondybey, *Nucl. Instr. Meth. B* **435**, 38 (2018).
21. Sasan Esmaili, Andrew D. Bass, Pierre Cloutier, Léon Sanche, and Michael A. Huels, *J. Chem. Phys.* **147**, 224704 (2017).
22. K.I. Öberg, E.F. van Dishoeck, H. Linnartz, and S. Andersson, *Astrophys. J.* **718**, 832 (2010).
23. J.B. Bossa, D.M. Paardekooper, K. Isokoski, and H. Linnartz, *Phys. Chem. Chem. Phys.* **17**, 17346 (2015).
24. R. Dupuy, M. Bertin, G. Féraud, X. Michaut, P. Jeseck, M. Doronin, L. Philippe, C. Romanzin, and J.-H. Fillion, *Astronomy & Astrophysics A* **603**, A61 (2017).
25. J.M. Carpenter, *Nature* **330**, 358 (1987).
26. T.L. Scott, J.M. Carpenter, and M.E. Miller, *Preprint ANL/IPNS/CP-98533* (1999).
27. E. Kulagin, S. Kulikov, V. Melikhov, and E. Shabalin, *Nucl. Instrum. Methods Phys. Res. B* **215**, 181 (2004).
28. O. Kirichek, C.R. Lawson, D.M. Jenkins, C.J.T. Ridley, and D.J. Haynes, *Cryogenics* **88**, 101 (2017).
29. O. Kirichek, E.V. Savchenko, C.R. Lawson, I.V. Khyzhniy, D.M. Jenkins, S.A. Uyutnov, M.A. Bludov, and D.J. Haynes, *J. Phys.: Conf. Ser.* **969**, 012006 (2018).
30. E.V. Savchenko, O. Kirichek, C.R. Lawson, I.V. Khyzhniy, S.A. Uyutnov, and M.A. Bludov, *Nucl. Instrum. Methods Phys. Res. B* **433**, 23 (2018).
31. I. Khyzhniy, S. Uyutnov, M. Bludov, and E. Savchenko, *Fiz. Nizk. Temp.* **44**, 1565 (2018) [*Low Temp. Phys.* **44**, 1223 (2018)].
32. E. Savchenko, I. Khyzhniy, S. Uyutnov, M. Bludov, G. Gumenchuk, and V. Bondybey, *Effects induced by electron beam in methane ices* (2018).
33. K.S. Song and R.T. Williams, *Self-Trapped Excitons*, Springer-Verlag, Berlin (1996).
34. Rob van Harrevelt, *J. Chem. Phys.* **126**, 204313 (2007).
35. *Vibrational Spectroscopy of Trapped Species*, H.E. Hallam (ed.), John Wiley & Sons, London (1973).
36. A. Chamberland, R. Belzile, and A. Cabana, *Can. J. Chem.* **48**, 1129 (1970).
37. G.B. Gumenchuk, M.A. Bludov, and A.G. Belov, *Fiz. Nizk. Temp.* **31**, 237 (2005) [*Low Temp. Phys.* **31**, 179 (2005)].
38. M. Kraas and P. Gurtler, *Chem. Phys. Lett.* **174**, 396 (1990).

39. E.V. Savchenko, I.V. Khyzhniy, S.A. Uytunov, G.B. Gumenchuk, A.N. Ponomaryov, M.K. Beyer, and V.E. Bondybey, *Fiz. Nizk. Temp.* **36**, 512 (2010) [*Low Temp. Phys.* **36**, 407 (2010)].
40. I.Ya. Fugol, A.G. Belov, E.V. Savchenko, and Yu.B. Poltoratskin, *Fiz. Nizk. Temp.* **1**, 203 (1975) [*Sov. Low Temp. Phys.* **1**, !!! (1975)].
41. D.E. Grosjean, R.A. Vidal, R.A. Baragiola, and W.L. Brown, *Phys. Rev. B* **56**, 6975 (1997).
42. Y. Tanaka and K. Yoshino, *J. Chem. Phys.* **53**, 2012 (1970).
43. T.E. Stewart, *J. Opt. Soc. America* **60**, 1290 (1970).
44. W. Krötz, A. Ulrich, B. Busch, G. Ribitzki, and J. Wieser, *Phys. Rev. A* **43**, 6089 (1991).
45. A.M. Boichenko, V.F. Tarasenko, S.I. Yakovlenko, *Las. Phys.* **9**, 1004 (1999).
46. T. Heindl, M. Dandl, R. Hofmann, L. Krücken, W. Oberauer, J. Potzel, J. Wieser, and A. Ulrich, *Europhys. Lett.* **91**, 62002 (2010).
47. V.I. Feldman, F.F. Sukhov, and A.Y. Orlov, *J. Chem. Phys.* **128**, 214511 (2008).
48. G.K. Oserov, D.S. Bezrukov, and A.A. Buchachenko, *Fiz. Nizk. Temp.* **45**, 347 (2019) [*Low Temp. Phys.* **45**, 301 (2019)].
49. L.B. Knight, Jr., W.E. Rice, L. Moore, E.R. Davidson, and R.S. Dailey, *J. Chem. Phys.* **109**, 1409 (1998).
50. V.I. Sugakov, *Lectures in Synergetics, World Scientific Series on Nonlinear Science*, Vol. 33, World Scientific, Singapore (1998).

### Індукована електронами затримана десорбція твердого аргону, допованого метаном

І.В. Хижний, С.А. Уютнов, М.А. Блудов,  
О.В. Савченко, В.Е. Bondybey

Вивчено інтегральний вихід часток із допованого метаном твердого аргону під дією електронів при температурі 5 К. Виміри виконано при концентраціях  $\text{CH}_4$  1% та 5%. Виявлено ефект вибухової затриманої десорбції з поверхні аргонної матриці для обох сумішей. Зі збільшенням концентрації  $\text{CH}_4$  він починався при менших дозах і був яскравіше виражений. Спостерігалось два типи автоколевань: довгоперіодичні (на шкалі часу близько 25 хв) і короткоперіодичні (близько 10 с). В чистому аргоні затримана десорбція не спостерігалась, незважаючи на накопичення значної кількості надлишкових електронів, що перевищує їх число в сумішах аргону з метаном, як було знайдено по термостимульованій екзоелектронній емісії. Ці результати виключають модель кулонівського вибуху для виявленого явища. Розглядається роль водню — одного з продуктів радіолізу метану — в явищі затриманої десорбції. Утворення атомарного водню в матриці відстежувалося за смугою випромінювання ексимеру  $\text{Ar}_2\text{H}^*$  при 166 нм. Виявлено десорбцію збуджених атомів водню по смузі  $\text{Lu-}\alpha$ . Виявлено зменшення інтенсивності

смуги  $\text{Ar}_2\text{H}^*$  при більшій концентрації  $\text{CH}_4$ , що свідчить про зменшення числа Н-центрів, очевидно, внаслідок їх рекомбінації з виділенням енергії та утворенням молекулярного водню. Отримані дані дають додатковий доказ на користь гіпотези, що екзотермічні реакції продуктів радіолізу є стимулюючим фактором для затриманої десорбції.

Ключові слова:  $\text{CH}_4$  в  $\text{Ar}$  матриці, електронне опромінення, вибухова затримана десорбція, катодолімінесценція, автоколевання.

### Индукцированная электронами задержанная десорбция твердого аргона, допированного метаном

И.В. Хижный, С.А. Уютнов, М.А. Блудов,  
Е.В. Савченко, В.Е. Bondybey

Изучен общий выход десорбции частиц из допированного метаном твердого аргона под действием электронов при температуре 5 К. Измерения выполнены при концентрациях  $\text{CH}_4$  1% и 5%. Обнаружен эффект взрывной задержанной десорбции с поверхности аргонной матрицы для обеих смесей. С увеличением концентрации  $\text{CH}_4$  он начинался при меньших дозах и был ярче выражен. Наблюдались два типа автоколебаний: долгопериодические (на шкале времени около 25 мин) и короткопериодические (около 10 с). В чистом аргоне задержанная десорбция не наблюдалась, несмотря на накопление значительного числа избыточных электронов, превышающего их число в смесях аргона с метаном, как было найдено по термостимулированной экзоелектронной эмиссии. Эти результаты исключают модель кулоновского взрыва для обнаруженного явления. Рассматривается роль водорода — одного из продуктов радиолиза метана — в задержанной десорбции. Образование атомарного водорода в матрице отслеживалось по полосе излучения эксимера  $\text{Ar}_2\text{H}^*$  при 166 нм. Обнаружена десорбция возбужденных атомов водорода по полосе  $\text{Lu-}\alpha$ . Обнаружено уменьшение интенсивности полосы  $\text{Ar}_2\text{H}^*$  при большей концентрации  $\text{CH}_4$ , что свидетельствует об уменьшении числа Н-центров, по-видимому, вследствие их рекомбинации с выделением энергии и образованием молекулярного водорода. Полученные данные дают дополнительное доказательство в пользу гипотезы, что экзотермические реакции продуктов радиолиза служат стимулирующим фактором для задержанной десорбции.

Ключевые слова:  $\text{CH}_4$  в  $\text{Ar}$  матрице, электронное облучение, взрывная задержанная десорбция, катодолімінесценція, автоколебания.